Spatial Characterization of the Uplink Inter-Cell Interference in Polygonal-Shaped Wireless Networks

Konstantinos B. BALTZIS

RadioCommunications Laboratory, Dept. of Physics, Aristotle University of Thessaloniki, Thessaloniki, Greece

kbaltzis@auth.gr

Abstract. *The uplink inter-cell interference is a major impairment in wireless systems. In this paper, we provide a geometrical-based framework for its analysis in networks with convex polygonal coverage area. Algebraic expressions for the Angle-of-Arrival (AoA) statistics of the uplink interfering signals are obtained. Simulation results validate the model. Representative examples show the dependence of the AoA on system geometry and demonstrate the relation between uplink interference and the radiation pattern of the receiver antenna. The proposed model is a generalization of previous studies in simpler geometries. It is a useful tool for the design, simulation and performance evaluation of wireless communication systems. The obtained expressions simplify the analysis of wireless networks and reduce the complexity and computational cost of their modeling and simulation.*

Keywords

Angle-of-Arrival, polygon, interference, radiation pattern, geometric modeling, wireless networks.

1. Introduction

Uplink (UL) interference is a major performance degradation factor in wireless communications [1], [2]. It usually deduces from the non-coherent summation at the desired unit, e.g. a base station (BS), of interfering signals from nodes that are served by this unit or nodes served by other ones, intra- and inter-cell interference, respectively, or from the coexistence of networks that operate in the same frequency band [3], [4]. UL interference increases with node density and transmission rate and reduces system capacity and the quality of service (QoS) levels.

The development of models that describe UL interference has been of interest since the very early stages of the development of wireless communications [1], [2], [5]-[12]. The author in [1] assumed a hexagonal cellular layout with aligned the closest edges of the cells. He provided simple closed-form expressions for the AoA distribution of the uplink interfering signals and explored the impact of cell sectorization and BS antenna radiation pattern on system capacity. An extension of this work for arbitrary hexagonal layouts was provided in a recent study [10]. The use of the moment-matching method and the application of the spatial Poisson process theory in the modeling of the spatial randomness of the interfering nodes allowed the description of first-, second- and zero-tier intercell interference in [2]. The authors in [5] assumed a circular node distribution and provided useful results for the statistics of the AoA of the uplink interfering signals that allowed the description of cochannel interference in the uplink of a cellular system. The model in [6] considered intracell and intercell log-normal shadowing, Rayleigh fading and diversity reception. In that study, it was found that the received signals in the uplink of a narrowband TDMA system could be modeled as Gaussian variables if they were conditioned on shadowing, transmitter(s) position and data sequences. Somekh et al. [7] proposed a simple Wyner-like multi-cell model with cells arranged in a circle and derived analytical expressions for the sum-rate capacities in intra-cell TDMA scheduling. The accuracy of Wyner-like models was also investigated in [11] where it was shown that such models are valid in dense networks but they fail for small number of active nodes. A 3-D geometric stochastic model for the study of cochannel interference in cellular systems was suggested in [8]. That model considered signal spread in both azimuth and elevation planes and allowed the investigation of the impact of antenna beam tilting on UL interference rejection. A stochastic geometry framework was also provided in [9] and allowed the description of UL interference and outage probability in two-tier femtocell networks considering power control and signal attenuation due to path loss and large-scale fading. According to the authors, their approach allowed the creation of an infrastructure for curbing cross-tier interference to increase UL capacity in shared spectrum networks. Recently [12], expressions for the UL interference statistics in cellular OFDMA networks under large-scale log-normal and small-scale Rayleigh shadowing were obtained and exhibited the significance of the modulation scheme, esp. for large code frame lengths such the ones suggested in the IEEE 802.16 standards [13].

Nowadays, complex models and powerful computer-aided analysis tools are common in the study and analysis of UL interference. However, in order to reduce the required complexity and computational cost for the characterization and description of networks performance, several

research attempts target to its analytical description. Geometric models fulfill these requirements by describing signal propagation in a simple but adequate way. These models idealize signal reception via a geometric abstraction of the spatial relationships among the communicating nodes. Commonly used in the modeling of the wireless propagation channel, e.g. [14]-[16], their simplicity and low computational cost have also made them popular in interference modeling [1], [5], [8]-[10], [17], [18].

It has to be noticed, that UL interference depends on the shape of the network area. In practice, the coverage area of a wireless network is irregularly shaped and influenced by man-made structures and terrain contour. However, approximate methods are suggested for analytical convenience. Common approaches are: the circular-shaped networks [5]-[8], [17], [19] that rise from the fact that the coverage area of omni-directional transmitters is, ideally, a circular disk; the hexagonal one [1], [2], [4], [9], [10], [12] which allows the full coverage of the network area; the rectangular approach [20]-[22] that is suitable for small-scale networks in indoor environments; the rhombus approximation [22], [23] which may be used when directional antennas are employed; the polygonal approach which is popular in wireless sensor networking [24]-[26] because the coverage area of these networks usually comprise Voronoi polygons [27]-[29] to assure reduced energy consumption and full network coverage.

In this paper, we develop an analytical framework for the calculation of the azimuth AoA of the incoming interfering signals at a fixed receiver. We extend previous works [1], [5], [10], and derive analytical expressions for the cumulative distribution function (cdf) and the probability density function (pdf) of the AoA of the uplink interfering signals from interferers distributed in a convex polygonal-shaped area. The obtained formulation is further used for the description of the spatial characteristics and the calculation of the outage probability of UL inter-cell interference. Comparisons with simulation results and notable models validate our proposal. Finally, we explore the relation between system geometry and AoA statistics and investigate the impact of the radiation pattern of the receiver antenna on system performance.

The proposed model suits for the design, analysis and simulation of polygonal-shaped networks. Applications can be found in areas such as wireless sensor and mobile ad hoc networking and in irregular (non-uniform) cellular systems but it can also be used in the study of regular-shaped networks with simple geometric layouts such as hexagonal, square and circular ones. The analytical description of the AoA statistics and UL interference simplifies the analysis and simulation of a wireless network and reduces the computational requirements. Moreover, the obtained formulation is more convenient than other approaches when network planning assumes *n*-gonal coverage areas.

The rest of the paper is organized as follows: Section 2 describes system geometry and modeling assumptions. In Section 3, we derive the mathematical formulation. Comparisons with simulation results and models in the literature are provided in Section 4. Section 5 presents numerical examples and applications in wireless networking. Finally, conclusions are drawn in Section 6.

2. System Geometry and Assumptions

We consider a polar coordinates system (let us call it system #1) with origin at a fixed reference point O, a convex *n*-gon with vertices at $P_i(\rho_i, \varphi_i)$, $i = 1,\ldots,n$, where $\varphi_{i+1} > \varphi_i$, and a point $O'(\rho_0, \varphi_0)$ outside the *n*-gon, see Fig. 1. It can be easily shown that the *i*th side of the *n*-gon, that is, the line segment with endpoints (ρ_i, φ_i) and $(\rho_{i+1}, \varphi_{i+1})$ (it is $\rho_{n+1} = \rho_1$ and $\varphi_{n+1} = \varphi_1$) is expressed as

$$r_i(\varphi) = \frac{\rho_{i+1}\rho_i \sin(\varphi_{i+1} - \varphi_i)}{\rho_{i+1}\sin(\varphi_{i+1} - \varphi) + \rho_i \sin(\varphi - \varphi_i)}, \quad \varphi \in [\varphi_i, \varphi_{i+1}]. \quad (1)$$

In order to develop our model, we neglect the vertical spreading of the propagating waves and consider a single line-of-sight signal path between each interferer and O' (single-bounce model).

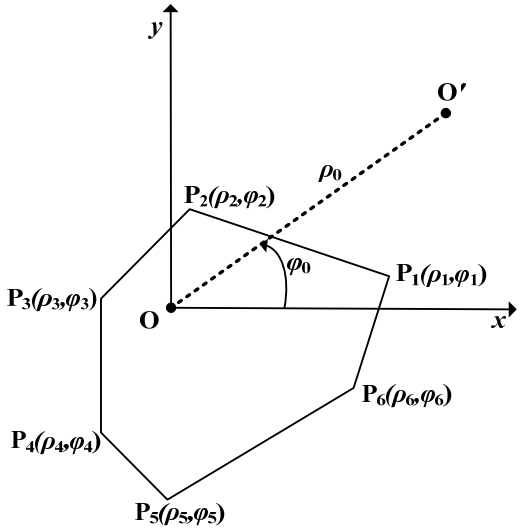

Fig. 1. System geometry; an irregular hexagon scenario.

3. Mathematical Formulation

This section consists of two parts. In the first, we derive the analytical formulation for the AoA pdf and cdf of the uplink interfering signals due to interferers that are uniformly distributed within a convex *n*-gonal region, at a receiver outside the *n*-gon. Next, we present simple well-known formulas for the probability of the UL inter-cell interference so as to improve the clarity of the presentation.

3.1 Derivation of the Uplink AoA Statistics

In order to develop our model, we set the origin of a new polar coordinates system (we call it system #2) at O'

and the point O at (ρ_0, φ_0). The coordinates of the ith vertex of the n-gon in systems #1 and #2, (ρ_i, φ_i) and (ρ_i', φ_i'), respectively, are related as:

$$\begin{aligned} \rho_i'\cos\varphi_i' &= \rho_i\cos\varphi_i - \rho_0\cos\varphi_0 \\ \rho_i'\sin\varphi_i' &= \rho_i\sin\varphi_i - \rho_0\sin\varphi_0 \end{aligned} \tag{2}$$

The solution of this system gives the new coordinates as:

$$\rho_i' = \sqrt{\rho_i^2 + \rho_0^2 - 2\rho_i\rho_0\cos(\varphi_i - \varphi_0)}, \tag{3}$$

$$\varphi_i' = \operatorname{atan}\left(\frac{\rho_i\sin\varphi_i - \rho_0\sin\varphi_0}{\rho_i\cos\varphi_i - \rho_0\cos\varphi_0}\right). \tag{4}$$

Substitution of (3) and (4) in (1) provides the expressions of the n-gon's sides $r_i'(\varphi')$ in system #2 (obviously, the transformation can be applied to all points in the 2D plane).

Based on the assumptions in Section 2, the probability of the AoA of the uplink interfering signals at O' due to the interferers within the n-gon, is proportional [1], [5], [10] to the area of the overlap between the region $\mathbf{C} = \{(x', y') \in \mathbf{R}^2 : \varphi'_{\min} \le \operatorname{atan}(y/x) \le \varphi'\}$ that is defined from the rays $\varphi'_{\min}$ and φ' with tip at O', and the n-gon (dark shaded region in Fig. 2).

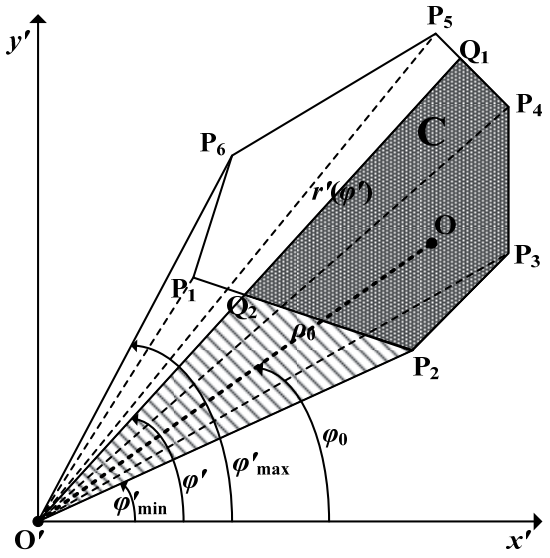

Fig. 2. Calculation of the AoA distribution of the uplink interfering signals.

The area of the overlapping region is obtained from the summation of n terms that are related to the triangles with tip at O' and opposite side each of the n-gon's sides. The absolute value of each term is the area of the overlap between the corresponding triangle and region **C** while its sign depends on system geometry. For example, in the case illustrated in Fig. 2, the desired area is the area of the triangles $O'P_2P_3$, $O'P_3P_4$ and $O'P_4Q_1$ minus the area of the $O'P_2Q_2$ triangle.

Since the interfering nodes are uniformly distributed within the n-gon, the cdf of the AoA equals to the product of the area of the overlapping region and the density of the interferers [1], [5], [10]; the last is inversely proportional to the area of the n-gon. Thus, the AoA cdf is

$$F(\varphi') = \frac{2\sum_{i=1}^{N} A_i(\varphi')}{\sum_{i=1}^{N}\rho_i'\rho_{i+1}'\sin(\varphi_{i+1}' - \varphi_i')} \tag{5}$$

where the quantity $\sum_{i=1}^{N}\rho_i'\rho_{i+1}'\sin(\varphi_{i+1}' - \varphi_i')$ is twice the n-gon area and

$$A_i(\varphi') = \begin{cases} 0, & \varphi' < \varphi'_{i,\min} \\ \dfrac{1}{2}\operatorname{sgn}(\varphi_{i+1}' - \varphi_i')\rho_{i_0}' \\ \times r_i'(\varphi')\sin(\varphi' - \varphi_{i0}') & , \ \varphi' \in [\varphi'_{i,\min}, \varphi'_{i,\max}] \\ \dfrac{1}{2}\rho_i'\rho_{i+1}'\sin(\varphi_{i+1}' - \varphi_i'), & \varphi' > \varphi'_{i,\max} \end{cases} \tag{6}$$

with $\varphi'_{i,\min} = \min(\varphi_i', \varphi_{i+1}')$ and $\varphi'_{i,\max} = \max(\varphi_i', \varphi_{i+1}')$. The index i_0 is equal to i when $\varphi_i' < \varphi_{i+1}'$; otherwise, it is $i_0 = i + 1$.

The AoA pdf $f(\varphi')$ is the derivative of $F(\varphi')$. The differentiation of (5) with respect to φ' gives, after some algebraic manipulation, that

$$f(\varphi') = \frac{\sum_{i=1}^{N} r_i'(\varphi')^2\, u(\varphi'; \varphi_i', \varphi_{i+1}')}{\sum_{i=1}^{N}\rho_i'\rho_{i+1}'\sin(\varphi_{i+1}' - \varphi_i')} \tag{7}$$

where

$$u(x; x_1, x_2) = \begin{cases} \operatorname{sgn}(x_2 - x_1), & x \in \left[\min_{i=1,2}(x_i), \max_{i=1,2}(x_i)\right] \\ 0, & \text{otherwise} \end{cases} \tag{8}$$

3.2 Expressions for the Uplink Inter-Cell Interference Probability

The amount of overlap in the angular domain between the radiation pattern of a receiving antenna and the spread of an incoming signal from an undesired source is a measure of the degree of UL interference from this source [5]. Thus, the convolution between the radiation pattern of the receiver antenna at O' and $f(\varphi')$ gives the probability $P(\varphi')$ that an interferer within the n-gon interferes at the angle φ' [1], [5], [8], [10]. For N interfering sources, the probability $P(\varphi' \mid M)$ that $M \le N$ sources interfere at φ' is the sum of all the products of the probability that M sources interfere at φ' by the probability that the remaining $N - M$ do not [5].

In order to achieve adequate signal reception, the desired signal power should be higher than the minimum required signal power level at the receiver input. Moreover, the desired signal should be stronger than interference by a margin known as interference protection ratio. In wireless communications, a measure of system performance is the outage probability. In general, this performance metric represents the probability of failing to achieve adequate signal reception. It may be defined as the average prob-

ability that the desired signal power does not exceed the interference power by a given protection ratio γ which equals to the minimum value of the wanted-to-unwanted signal ratio at the receiver input so as to achieve a specified reception quality at the receiver output. In our case, the outage probability is obtained [5], [8], from the expression

$$P(CIR<\gamma)=\sum_{M=1}^{N}P(Z<0\,|\,M)\overline{P(\varphi'\,|\,M)} \qquad (9)$$

with CIR the carrier-to-interference ratio, $Z=CIR-\gamma$ the carrier-to-interference plus protection ratio (in dB), $P(\varphi'\,|\,M)$ the average $P(\varphi'\,|\,M)$ over φ', and $P(Z<0\,|\,M)$ the conditional probability of interference from M sources. The last term depends on the propagation medium [5], [8], [30]-[32]. For example, for non-coherent addition of interfering signals with equal received local mean power and propagation in a Rayleigh fading environment, it is approximated [31] as

$$P(Z<0\,|\,M)\approx 1-\left(1+10^{-Z/10}\right)^{-M}. \qquad (10)$$

4. Model Validation

In order to validate the proposed model, we performed simulations for different system geometries. Here, we show the results for a representative case. System parameters were chosen so as to verify the accuracy of the model in a complex scenario. In particular, we consider a convex heptagon with vertices coordinates specified in Tab. 1 (distances are normalized to the maximum ρ_i, $i=1,\ldots,n$). The r_0 and φ_0 are 0.6 and 50 deg, respectively.

i	1	2	3	4	5	6	7
ρ_i	0.3	0.6	0.9	1	0.6	0.6	0.4
φ_i (deg)	15	78	110	165	240	271	312

Tab. 1. Coordinates of the heptagon's vertices.

In each simulation run, a single node was randomly positioned within a unit circle centered at O. The random points in the n-gon were generated using the acceptance-rejection method [33]; in order to achieve this, we used (1) to express the sides of the n-gon in polar coordinates. In Appendix, the algorithm flowchart for the calculation of the AoA pdf is illustrated. The simulations ran on a HP Z200 SFF Workstation with Quad Core Intel Xeon™ at 2.4 GHz with 4GB RAM. The source code was written in Borland C++ Builder 5.0.

Fig. 3 shows the spatial distribution of the generated points for 10^4 snapshots. Next, Figs. 4 and 5 plot the analytical cdf and pdf curves calculated from (5) and (7), respectively, and the simulation results obtained from 10^6 independent runs. The simulated values were averaged over 2-deg intervals. The required computational time for the derivation of the AoA pdf and cdf simulated curves was 1.81 sec. We notice that the simulation results closely match theory.

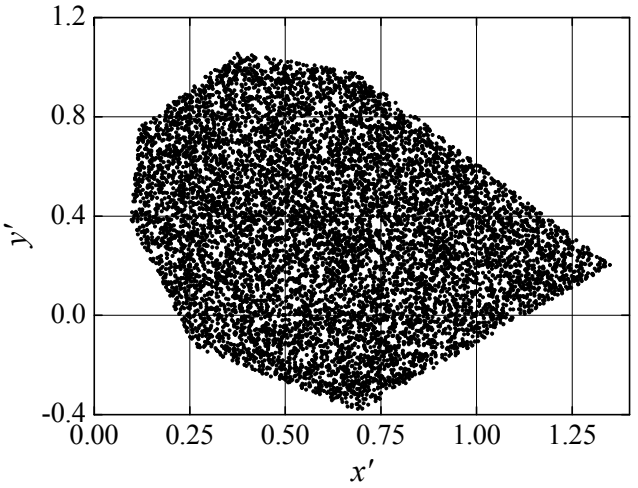

Fig. 3. Spatial distribution of the generated nodes.

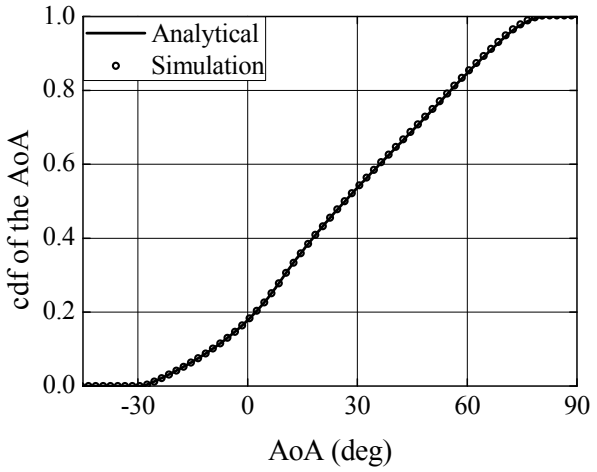

Fig. 4. AoA cdf of the uplink interfering signals; analytical curve and simulation results.

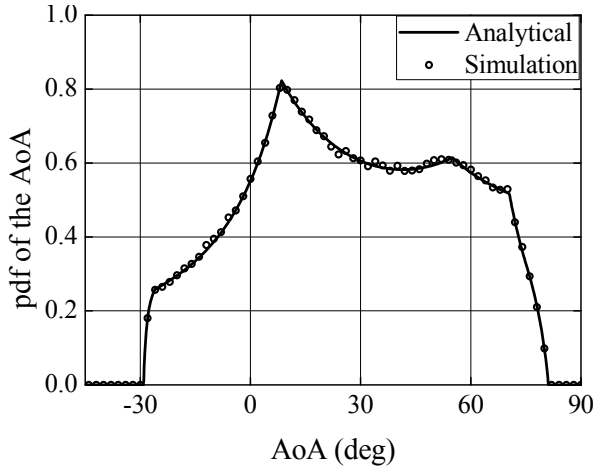

Fig. 5. AoA pdf of the uplink interfering signals; analytical curve and simulation results.

Our proposal extends previous models for the description of UL interference in regular-shaped networks. For example, the AoA cdf and pdf expressions in the circular-based model [5] are obtained from (5) and (7) by setting ρ_0 the distance between the BSs in the desired and the interfering cell, $\varphi_0=0$, $(\rho_i,\varphi_i)=(R,2\pi(i-1)/n)$,

$i = 1,\ldots,n$, with R the radius of the network and n a very large integer number. In the case of hexagonal cellular networks [10], we set $n = 6$, $\rho_{1\ldots6} = r$, where r is the circumradius of the cell, $\varphi_i = 60(i - 1)$, $i = 1,\ldots,6$, and ρ_0 is the distance between the BSs in the desired and the interfering cells. In this case, the value of ρ_0 depends on the reuse factor; moreover, the angle φ_0 is further related to the cell layout (see [34] for a detailed analysis and examples on the choice of these parameters).

5. Examples and Discussion

In this section, we first investigate the impact of system geometry on the AoA statistics of the UL interfering signals. Then, we study the relation between interference and antennas radiation pattern and apply the obtained formulation in the study of cochannel interference in a cellular network.

In Figs. 6 and 7, we see the relation between the UL AoA cdf and pdf and the receiver position. The interfering network is a heptagonal-shaped one with vertices coordinates given in Tab. 1. For the sake of clarity, the x-axis in the figures shows the AoA minus the φ_0 angle. Fig. 6 shows that the slope of the cdf curves increases with ρ_0 while the changes in φ_0 shift them along the polar axis; this shift reduces with the increment of ρ_0. Also, for a given φ_0, the cdf curves intersect at $\varphi' = \varphi_0$ for any ρ_0. It has to be noticed, that the complexity of the relation between the AoA cdf and φ_0 is due to the dependence of the first on the shape of the interfering network. The impact of receiver position on the AoA statistics is further highlighted from the study of the AoA pdf, see Fig. 7. As it was expected from system geometry, the pdf curves flatten as ρ_0 decreases while any change in the angle φ_0 shifts similarly the curves along the polar axis. The shape of the curves is also affected from φ_0. In particular, the pdf curves show peaks at φ_i' while their irregular shape is due to the irregularities in the shape of the interfering region.

In a wireless communication system, a measure of UL interference is the probability that a node interferes at the desired receiver. Fig. 8 illustrates the probability of UL inter-cell interference from a distant node, $P(\varphi)$, at receivers with omni-directional antennas and antennas with cosine-like radiation patterns [35], side-lobe level $SLL = -15$ dB and varied half-power beamwidth (HP) (typical radiation pattern characteristics of receiver antennas in cellular networks [36]). System geometry is similar to the example in Section 4. We notice that the probability that a node causes interference at a given angle increases with HP. Moreover, the receiver is more vulnerable to interference from nodes that are spread in a wide area when the half-power beamwidth of the receiving antennas increases. This behavior is attributed to the increase of the interfering signals that penetrate the main lobe of the antenna radiation pattern. Based on the above, we expect smaller performance degradation due to UL interference in narrow-beam systems (similar conclusions were drawn in [1], [5], [10]).

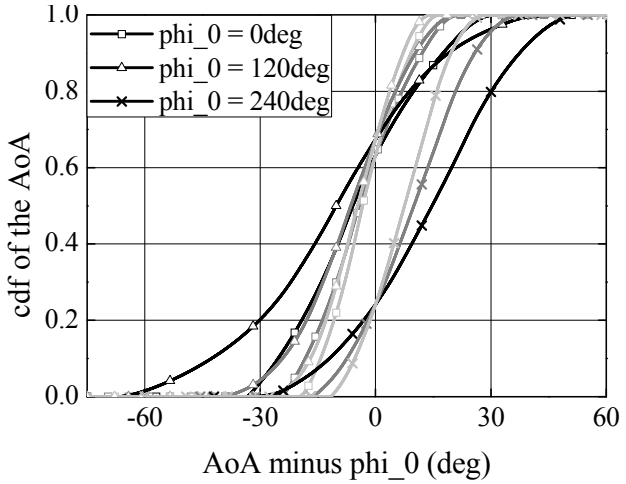

Fig. 6. Impact of receiver position on the AoA cdf ($\rho_0 = 1$: black curves; $\rho_0 = 1.5$: dark grey curves; $\rho_0 = 2$: light grey curves).

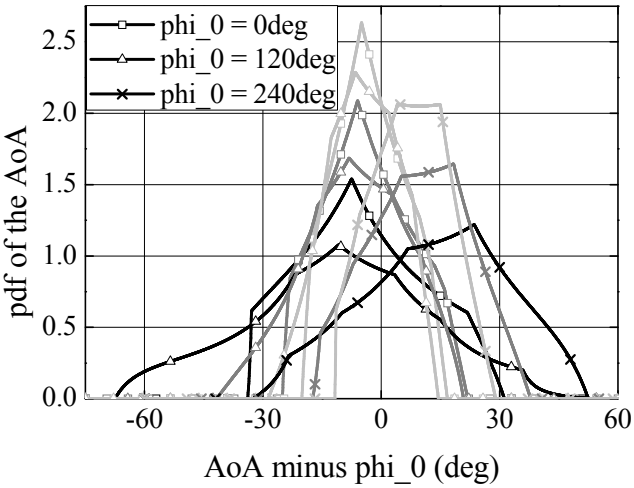

Fig. 7. Impact of receiver position on the AoA pdf ($\rho_0 = 1$: black curves; $\rho_0 = 1.5$: dark grey curves; $\rho_0 = 2$: light grey curves).

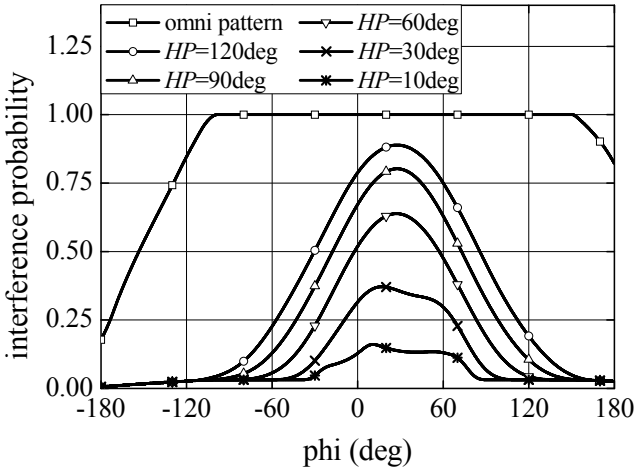

Fig. 8. $P(\varphi)$ versus φ in systems with different receiver antenna configurations.

As an application example, we study the dependence of UL cochannel interference on the BS antenna radiation pattern in a cellular system. We consider a hexagonal sin-

gle cluster network with the BSs centered at each cell. For simplicity, we neglect the interference from cells other than the first ring ones. We further consider Rayleigh fading only and assume that the mean received power from each interferer is the same. The receiving antennas are flat-top beamformers [5] with $SLL = -10$ dB. With no loss of generality, we set $\gamma = 8$ dB and the nodes activity level equal to 0.4. Fig. 9 plots the outage probability as a function of the receiving antennas beamwidth for different *CIR* values. Clearly, the outage probability increases significantly with beamformer beamwidth indicating the advantages of sectorization and the use of narrow-beam antennas. Apart from this, this performance degradation increases with *CIR*.

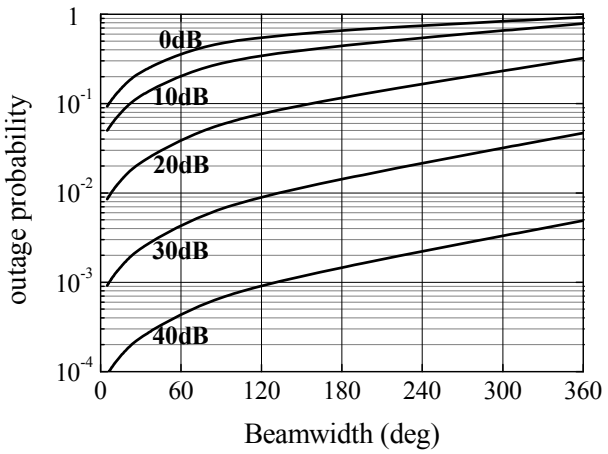

Fig. 9. Outage probability as a function of the beamformer beamwidth for *CIR* equal to 0, 10...40 dB.

Now, let us consider a UMTS system with hexagonal single cluster cellular layout. For the sake of convenience, we assume that the system is interference limited. The authors in [39] were based on the technical report 3GPP TR 23.907 v1.2.0 [37] (similar outcomes have been reached in the technical specification 3GPP TS 23.107 v11.0.0 [38]) and suggested that a maximum acceptable outage probability in the uplink of a WCDMA cellular system is equal to 10^{-2} for voice and video and 10^{-3} for web-browsing and data transmission services. From Fig. 9 comes that in the first case, a *CIR* greater than 20 dB is required, even in systems with narrow-beam antennas; when we use antennas with beamwidth greater than 120 deg the *CIR* should be increased by at least 10 dB. In order to support web–browsing and data transmission services, antennas with beamwidth less than 120 deg and a *CIR* greater than 40 dB are requisite.

It has to be noticed that the application of the proposed model is limited in narrowband communication systems and/or flat fading propagation environments. In particular, (5) and (7) are frequency-independent quantities; however, several studies, e.g. [40]-[42], have shown a dependence of the angular spread of radio signals on signal frequency. However, the proposed model can provide a framework for a more sophisticated and extensive analysis that includes additional issues such as the frequency dependence. For example, in the geometric modeling of the wireless medium, single cluster and/or single ray concepts are often extended to multi-cluster and multi-ray models so as to describe wideband and/or frequency-selective propagation channels [43], [44]. A similar approach could be followed here by considering multiple arriving paths from each interferer at the receiver front end (multi-bounce model).

6. Conclusions

In this paper, we proposed a geometrical-based stochastic model for the calculation of the AoA of the uplink interfering signals in networks with polygonal-shaped coverage areas. Our approach is a generalization of simpler models in the literature. Analytical expressions for the statistics of the AoA of the uplink inter-cell interfering signals were derived. Simulation results validated the proposal. We investigated the impact of system geometry on the AoA statistics and showed the importance of the radiation pattern of the receiver antenna on UL interference rejection. The main contribution of this work is the consideration of polygonal-shaped networks. The analytical description of the AoA statistics assists in network planning, design and performance evaluation and reduces the requirements of system-level simulations.

Appendix

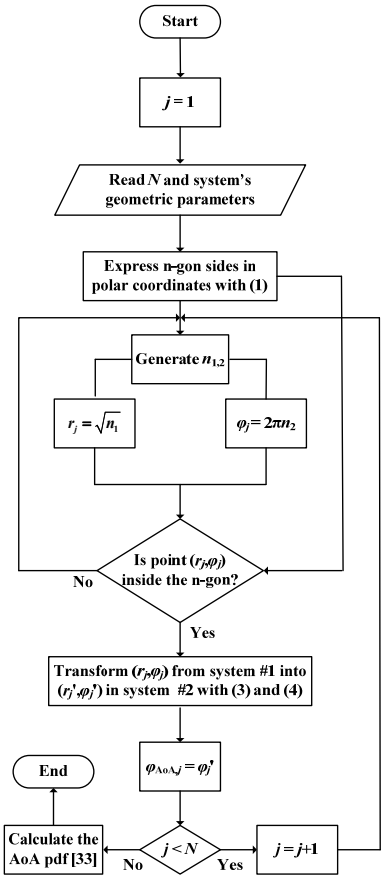

Fig. A1. Flowchart of the simulation algorithm.

In this Appendix, we illustrate the flowchart of the AoA pdf curve simulation algorithm. Parameter N represents the number of simulation runs, $n_{1,2}$ are random numbers uniformly distributed in the range [0,1] and $\varphi_{\mathrm{AoA},j}$, $j = 1,\ldots,N$, is the calculated value of the uplink AoA in the jth iteration. The AoA cdf is directly obtained from the calculated pdf values [33].

References

[1] BALTZIS, K. B. A geometrical-based model for cochannel interference analysis and capacity estimation of CDMA cellular systems. *EURASIP Journal on Wireless Communications and Networking,* 2008, 7 pages, doi: 10.1155/2008/791374.

[2] SINGH, S., MEHTA, N. B., MOLISCH, A. F., MUKHOPADYHAY, A. Moment-matched lognormal modeling of uplink interference with power control and cell selection. *IEEE Transactions on Wireless Communications,* 2010, vol. 9, no. 3, p. 932 - 938.

[3] GLEISSNER, F., HANUS, S. Co-channel and adjacent channel interference measurement of UMTS and GSM/EDGE systems in 900 MHz radio band. *Radioengineering*, 2008, vol. 17, no. 3, p. 74 to 80.

[4] YUN, J.-H., SHIN, K. G. Adaptive interference management of OFDMA femtocells for co-channel deployment. *IEEE Journal on Selected Areas in Communications*, 2011, vol. 29, no. 6, p. 1225 to 1241.

[5] PETRUS, P., ERTEL, R. B., REED, J. H. Capacity enhancement using adaptive arrays in an AMPS system. *IEEE Transactions on Vehicular Technology*, 1998, vol. 47, no. 3, p. 717 - 727.

[6] GRANT, S. J., CAVERS, J. K. System-wide capacity increase for narrowband cellular systems through multiuser detection and base station diversity arrays. *IEEE Transactions on Wireless Communications*, 2004, vol. 3, no. 6, p. 2072 - 2082.

[7] SOMEKH, O., ZAIDEL, B. M., SHAMAI, S. Sum rate characterization of joint multiple cell-site processing. *IEEE Transactions on Information Theory*, 2007, vol. 53, no. 12, p. 4473 - 4497.

[8] BALTZIS, K. B., SAHALOS, J. N. A low–complexity 3-D geometric model for the description of CCI in cellular systems, *Electrical Engineering (Archiv für Elektrotechnik)*, 2009, vol. 91, no. 4, p. 211 - 219.

[9] CHANDRASEKHAR, V., ANDREWS, J. G. Uplink capacity and interference avoidance for two-tier femtocell networks. *IEEE Transactions on Wireless Communications*, 2009, vol. 8, no. 7, p. 3498 - 3509.

[10] BALTZIS, K. B., SAHALOS, J. N. On the statistical description of the AoA of the uplink interfering signals in a cellular communication system. *European Transactions on Telecommunications*, 2010, vol. 21, no. 2, p. 187 - 194.

[11] XU, J., ZHANG, J., ANDREWS J. G. On the accuracy of the Wyner model in cellular networks. *IEEE Transactions on Wireless Communications*, 2011, vol. 10, no. 9, p. 3098 - 3109.

[12] SAGONG, M, CHEUN, K. A statistical inter-cell interference model for uplink cellular OFDMA networks under log-normal shadowing and Rayleigh fading. *IEEE Communications Letters*, 2012, vol. 16, no. 6, p. 824 - 827.

[13] DEMİR, M. A., OZEN, A. A novel variable step size adjustment method based on autocorrelation of error signal for the constant modulus blind equalization algorithm. *Radioengineering*, 2012, vol. 21, no. 1, p. 37 - 45.

[14] NAWAZ, S. J., KHAN, N. M., PATWARY, M. N., MORINI, M. Effect of directional antenna on the Doppler spectrum in 3-D mobile radio propagation environment. *IEEE Transactions on Vehicular Technology*, 2011, vol. 60, no.7, p. 2895 - 2903.

[15] BALTZIS, K. B. A simplified geometric channel model for mobile-to-mobile communications. *Radioengineering*, 2011, vol. 20, no. 4, p. 961 - 967.

[16] OLENKO, A. Y., WONG, K. T., QASMI, S. A. Distribution of the uplink multipaths' arrival delay and azimuth-elevation arrival angle because of 'bad urban' scatterers distributed cylindrically above the mobile. *Transactions on Emerging Telecommunications Technologies*, 2012, 20 pages, doi: 10.1002/ett.2530.

[17] ZHANG, Z., WEI, S., YANG, J., ZHU, L. CIR performance analysis and optimization of a new mobile communication cellular configuration. In *Proceedings of the 4th International Conference on Microwave and Millimeter Wave Technology*. Beijing (China), 2004, p. 826 - 829.

[18] ZHANG, Z., LEI, F., DU, H. More realistic analysis of co-channel interference in sectorization cellular communications systems with Rayleigh fading environments. In *Proceedings of the 2nd International Conference on Wireless Communications, Networking and Mobile Computing*. Wuhan (China), 2006, 5 pages, doi: 10.1109/WiCOM.2006.184.

[19] XIAO, L., GREENSTEIN, L., MANDAYAM, N., PERIYALWAR, S. Distributed measurements for estimating and updating cellular system performance. *IEEE Transactions on Communications*, 2008, vol. 56, no.6, p. 991 - 998.

[20] PIRINEN, P. Outage analysis of ultra-wideband system in log-normal multipath fading and square-shaped cellular configurations. *EURASIP Journal on Wireless Communications and Networking,* 2006, 10 pages, doi: 10.1155/wcn/2006/19460.

[21] ZHUANG, Y., PAN, J., CAI, L. Minimizing energy consumption with probabilistic distance models in wireless sensor networks. In *Proceedings of the 29th IEEE International Conference on Computer Communications*. San Diego (USA), 2010, 9 pages, doi: 10.1109/INFCOM.2010.5462073.

[22] ZHUANG, Y., PAN, J. A geometrical probability approach to location-critical network performance metrics. In *Proceedings of the 31st IEEE International Conference on Computer Communications*. Orlando (USA), 2012, p. 1817 - 1825.

[23] BAI, X., KUMAR, S., XUAN, D., YUN, Z., LAI, T. H. Deploying wireless sensors to achieve both coverage and connectivity. In *Proceedings of the 7th ACM International Symposium on Mobile Ad Hoc Networking and Computing*. Florence (Italy), 2006, p. 131 to 142.

[24] ISLAM, M. R. An issue of boundary value for velocity and training overhead using cooperative MIMO technique in wireless sensor network. *Radioengineering*, 2011, vol. 20, no. 2, p. 505 - 511.

[25] MORAVEK, P., KOMOSNY, D., SIMEK, M., GIRBAU, D., LAZARO, A. Energy analysis of received signal strength localization in wireless sensor networks. *Radioengineering*, 2011, vol. 20, no. 4, p. 937 - 945.

[26] SIMEK, M., MORAVEK, P., KOMOSNY, D., DUSIK, M. Distributed recognition of reference nodes for wireless sensor network localization. *Radioengineering*, 2012, vol. 21, no. 1, p. 89 to 98.

[27] MELODIA, T., POMPILI, D., AKYILDIZ, I. F. Handling mobility in wireless sensor and actor networks. *IEEE Transactions on Mobile Computing*, 2010, vol. 9, no.2, p. 160 - 173.

[28] NOORI, M., ARDAKANI, M. Lifetime analysis of random event-driven clustered wireless sensor networks. *IEEE Transactions on Mobile Computing*, 2011, vol. 10, no.10, p. 1448 - 1458.

[29] LI, W., MARTINS, P., SHEN, L. Determination method of optimal number of clusters for clustered wireless sensor networks. *Wireless Communications and Mobile Computing*, 2012, vol. 12, no. 2, p. 158 - 168.

[30] MUAMMAR, R., GUPTA, S. Cochannel interference in high-capacity mobile radio channels. *IEEE Transactions on Communications*, 1982, vol. 30, no. 8, p. 1973 - 1978.

[31] PRASAD, R., KEGEL, A. Improved assessment of interference limits in cellular radio performance. *IEEE Transactions on Vehicular Technology*, 1991, vol. 40, no. 2, p. 412 - 419.

[32] AU, W. S., MURCH, R. D., LEA, C. T. Comparison between the spectral efficiency of SDMA systems and sectorized systems. *Wireless Personal Communications*, 2001, vol. 16, no. 1, p. 51 to 67.

[33] PAPOULIS. A., PILLAI, S. U. *Probability, Random Variables and Stochastic Processes*. 4th ed. New York: McGraw-Hill, 2002.

[34] LEE, J. S., MILLER, L. E. *CDMA Systems Engineering Handbook*. Boston: Artech House, 1998.

[35] BALANIS, C. A. *Antenna Theory*. 3rd ed. Hoboken: Wiley, 2005.

[36] NIEMELÄ, J., ISOTALO, T., LEMPIÄINEN, J. Optimum antenna downtilt angles for macrocellular WCDMA network. *EURASIP Journal on Wireless Communications and Networking*, 2005, vol. 2005, no. 5, p. 816 - 827.

[37] 3G TR 23.907 v1.2.0. Quality of Service (QoS) concept. *DTS/TSGS-0223101U*, 1999.

[38] 3GPP TS 23.107 v11.0.0. Quality of Service (QoS) concept and architecture. *RTS/TSGS*-0223107vb00, rel. 11, 2012.

[39] NIE, C., WONG, T. C., CHEW, Y. H. Outage analysis for multi-connection multiclass services in the uplink of wideband CDMA cellular mobile networks. In *Proceedings of the 3rd IFIP-TC6 Networking Conference – Networking 2004*. Athens (Greece), 2004, p. 1426 - 1432.

[40] MALIK, W. Q., EDWARDS, D. J., STEVENS, C. J. Frequency dependence of fading statistics for ultrawideband systems. *IEEE Transactions on Wireless Communications*, 2007, vol. 6, no. 3, p. 800 - 804.

[41] MALIK, W. Q. Spatial correlation in ultrawideband channels. *IEEE Transactions on Wireless Communications*, 2008, vol. 7, no. 2, p. 604 - 610.

[42] PHAKASOUM, C., GHORAISHI, M., TAKADA, J.-I., KITAO, K., IMAI, T. Frequency characteristics of angular spread for radio wave propagation through foliage. In *Proceedings of the 5th European Conference on Antennas and Propagation*. Rome (Italy), 2011, p. 3289 - 3292.

[43] PÄTZOLD, M., HOGSTAD, B. O. A wideband MIMO channel model derived from the geometric elliptical scattering model. *Wireless Communications and Mobile Computing*, 2008, vol. 8, no. 5, p. 597 - 605.

[44] CHENG, X., WANG, C.-X., LAURENSON, D. I. A geometry-based stochastic model for wideband MIMO mobile-to-mobile channels. In *Proceedings of the 2009 IEEE Global Telecommunications Conference*. Honolulu (USA), 2009, 6 pages, doi: 10.1109/GLOVOM.2009.5425319.

About Author ...

Konstantinos B. BALTZIS holds a B.Sc. in Physics, a M.Sc. in Communications and Electronics and a Ph.D. in Wireless Communications. He is a research associate in the RadioCommunications Laboratory of the Aristotle University of Thessaloniki (AUTh) and an adjunct professor in the Postgraduate Studies in the Department of Physics at AUTh. Dr. Baltzis is an IEEE Senior Member and serves as a member of the editorial board of the Radioengineering journal and the Journal of Wireless Networking and Communications. He has published more than fifty papers in international peer-reviewed journals and conferences and contributed two book chapters. His current research interests are focused on wireless communication systems and networks, signal propagation, antennas design and evolutionary optimization methods.